



Investigation of Alumina Wetting by Fe-Ti, Fe-P and Fe-Ti-P Alloys

Augustin Karasangabo & Christian Bernhard

To cite this article: Augustin Karasangabo & Christian Bernhard (2012) Investigation of Alumina Wetting by Fe-Ti, Fe-P and Fe-Ti-P Alloys, Journal of Adhesion Science and Technology, 26:8-9, 1141-1156

To link to this article: <http://dx.doi.org/10.1163/016942411X580252>



Published online: 24 Jul 2012.



Submit your article to this journal [↗](#)



Article views: 50



View related articles [↗](#)

Investigation of Alumina Wetting by Fe–Ti, Fe–P and Fe–Ti–P Alloys

Augustin Karasangabo* and Christian Bernhard

Christian Doppler Laboratory for Metallurgical Fundamentals of Continuous Casting Processes,
Chair of Metallurgy, University of Leoben, Franz-Josef-Straße 18, A – 8700 Leoben, Austria

Received on 19 April 2011

Abstract

The wetting of alumina substrates by Fe–Ti, Fe–P and Fe–Ti–P alloys has been investigated using sessile drop experiments conducted under an inert gas atmosphere in the temperature range of 1550 to 1620°C. The surface and interfacial structures have been explored by scanning electron microscopy and energy dispersive X-ray spectroscopy.

Substantial additions of titanium are known to induce steel melts to wet alumina due to the formation of a Ti-rich reaction product at the alloy/ceramic interface, but the present work has shown that even low Ti concentrations can induce a reactive wetting process leading to an improvement of the wettability of alumina by Fe alloys. The contact angle of molten steel containing phosphorus on alumina decreased with increasing P content. The improvement of the wetting behaviour in this system was attributed solely to the adsorption of P onto the surface of the Fe melt. The addition of P as a ternary alloying element to the system Fe–Ti proved to be beneficial to the wetting behaviour. The measured contact angles were much lower than those in the binary systems Fe–Ti and Fe–P. This effect was related to the fact that P enhances the activity of Ti in the Fe melt.

According to experimental observations, it turns out that the wettability of liquid Fe-based alloys, when an Al₂O₃ surface is present, is not only a property of the metal/oxide couple but is also dependent on the oxygen partial pressure, whereas temperature variations bring about a comparatively small effect.

This work is of interest in understanding the phenomena pertaining to inclusion engineering and steel–refractory interactions, such as the clogging of submerged entry nozzles by agglomerated alumina particles during the continuous casting process.

© Koninklijke Brill NV, Leiden, 2012

Keywords

Adhesion, agglomeration, contact angle, continuous casting, clogging, drop shape analysis, non-metallic inclusions, sessile drop

* To whom correspondence should be addressed. Tel.: +4338424022252; Fax: +4338424022202; e-mail: augustin.karasangabo@unileoben.ac.at

1. Introduction

An understanding of iron alloy/refractory material interactions is important because these materials are extensively applied in a number of metallurgical processes. Typical examples related to the continuous casting process are the mechanisms of generation and removal from molten steel of non-metallic inclusions [1, 2], as well as their entrapment at the internal wall of the tube delivering steel into the mould, the so-called submerged entry nozzle, an adhesion process which can eventually lead to the clogging of the nozzle [1, 3].

Reactions between molten iron alloys and alumina-based materials have been the subject of a number of investigations [2, 4–7]. However, most of the efforts have been focused on pure Fe/Al₂O₃ systems or on Fe alloys containing extremely high concentrations (up to 30 mass percent or more) of the alloying element. The aim of the present study was to investigate the effect of titanium and phosphorus on wetting in the Fe-based alloy/Al₂O₃ couple on samples reasonably close to commercial steel compositions. The ultimate goal being to determine the role played by wetting properties of Fe alloys in the nozzle clogging mechanisms during the continuous casting of steels.

The motivation for the choice of alumina as substrate material was twofold: first, Al₂O₃ is an interesting ceramic material which constitutes one of the major components of the submerged entry nozzle used in the continuous casting process of steels; secondly, non-metallic inclusions formed in aluminium-killed steels are mainly composed of Al₂O₃. An understanding of the phenomena underlying the reactions in the Fe alloy/Al₂O₃ system would, therefore, be useful in optimising the continuous casting process.

Titanium and phosphorus contents were chosen as the experimental variables of the steel, since literature [8, 9] and operational experience show that the presence of these elements tends to exacerbate the problem of nozzle clogging during the continuous casting of Al-killed steels bearing Ti and/or P.

Generally, a liquid placed on a solid substrate forms a droplet which has a specific equilibrium shape and contact (wetting) angle. The equilibrium contact angle, θ , Fig. 1, which is a quantitative measure of the ability of a liquid to wet the substrate,

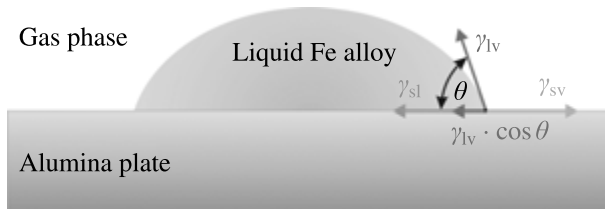


Figure 1. Schematic drawing of a liquid drop resting on a flat Al₂O₃ substrate in a partial wetting situation.

can be described by Young's equation [10], which is the result of balancing the force components at the three-phase line:

$$\gamma_{lv} \cdot \cos \theta = \gamma_{sv} - \gamma_{sl}, \quad (1)$$

where γ_{ij} denotes the interfacial tension of the interface ij and s, l and v designate the solid, liquid and gas phase, respectively.

A contact angle $\theta < 90^\circ$ indicates that the solid is wetted by the liquid, and $\theta > 90^\circ$ identifies a non-wetting behaviour, with the limits $\theta = 0^\circ$ and $\theta = 180^\circ$ defining complete wetting and complete non-wetting, respectively [11, 12]. Thus, the degree of interaction between the liquid and the substrate material increases as the contact angle decreases [13].

Following equation (1), an improvement in wetting can result either from a decrease of γ_{sl} only or from a decrease of both γ_{sl} and γ_{lv} . A change in interfacial tensions and thus in the wetting characteristics of the system Fe alloy/ Al_2O_3 can be brought about by one or a combination of the following parameters:

Surface Enrichment by Adsorption or Segregation

The surface and interfacial tensions of an Fe melt can be extremely lowered by the presence of minute amounts of interface active elements at the metal/vapour and/or at the refractory/metal interfaces [14–18]. The same phenomenon is observed during the alloying process, especially if the added solutes tend to segregate at the metal surface and at the refractory/metal interface [19]. Most additions to Fe produce a decrease of the interfacial tension, their influence being more pronounced in the following order: Ni, Mn, Cr, Mo, Si, P, C, V and Ti. Unlike this group, W belongs to the few elements that contribute to an increase of the interfacial tension between Fe-based alloys and oxide substrates [20]. The role of oxygen is of particular interest as this element is present in most steelmaking processes and because its surface active effect contributes to a considerable reduction of the values of γ_{ij} in liquid Fe/ceramic couples with increasing oxygen partial pressure. Nakashima *et al.* [21] investigated the effects of the oxygen partial pressure on the values of θ in the system Fe–O/ Al_2O_3 . They found that the contact angle θ versus the concentration X_{O} of dissolved oxygen curve passes through a maximum for $\theta = 130^\circ$ and $X_{\text{O}} \approx 50$ ppm. At oxygen contents lower than 50 ppm the contact angle decreases due to the increase of Al concentration following the dissolution of Al_2O_3 and the subsequent increase of the concentration of Al, an element that adsorbs at metal/oxide interfaces. And at oxygen contents higher than 50 ppm the contact angle decreases again due to oxygen adsorption. Moreover, a dense layer of hercynite is formed at the surface of the substrate. A similar behaviour was also found in a work by Ueda *et al.* [22].

Ridge Formation

For most high-temperature systems, the experimental temperatures are typically $\geq (0.2-0.5)T_m$, where T_m is the melting point of the substrate material, and, therefore, local atomic diffusion can occur [23]. This provides conditions for ridge

formation even for hard substrates like alumina as has been observed by Saiz *et al.* [24]. They demonstrated the formation of ridges during wetting experiments of liquid metals on Al_2O_3 substrates. Carré and Shanahan [25] found out that the effect of a ridge consists in slowing down, even stopping, the spreading of a metal on the ceramic. De Jonghe and Chatain [26] observed that ridges, in pinning the triple line, have an influence on the value of the equilibrium wetting angle.

Interfacial Reactions

In a non-reactive system, the nature of the ceramic substrate is not significantly modified by its contact with a metal melt. The wettability is only the result of chemical bonds which are achieved by the mutual saturation of the free valences of the contacting surfaces and acting van der Waals forces [14, 27]. Therefore, the interaction of liquid metal with the ceramic does not lead to the formation of new phases. In reactive systems, however, wetting, chemical reactions and solute segregation are interactively coupled [28]. The liquid metal is not in direct contact with the initial unreacted substrate, but with the new compound formed at the metal/ceramic interface due to the chemical reaction accompanying the wetting process [15, 19]. In this case, the final wetting angle θ_f may be expressed by the Young's equation applied to the reaction product/liquid/gaseous system [14]:

$$\cos \theta_f = \frac{\gamma_{pv} - \gamma_{pl}}{\gamma_v} \quad (2)$$

in which θ_f represents the equilibrium wetting angle on the reaction product p .

Obviously, the wetting in reactive systems is governed by the final interfacial chemistry at the triple line rather than by the intensity of interfacial reactions [29–31]. This means that even a very thin reaction layer may profoundly affect the wetting behaviour [32].

2. Experimental Method

The sessile drop technique was used in the present study to measure the contact angles of molten Fe alloys containing Ti and P on solid Al_2O_3 substrates as a function of the alloy chemical composition at temperatures ranging from 1550 to 1620°C.

2.1. Sample Preparation for Wetting Tests

In order to reduce the contamination of the Fe alloys with oxygen to minimal levels, the master alloys were prepared using a novel method consisting in a combination of vacuum induction melting and air induction melting with a $\text{CaO-SiO}_2\text{-Al}_2\text{O}_3$ protective slag, as well as sampling done under an inert gas atmosphere [33].

Table 1 shows the chemical composition of all Fe–Ti, Fe–P and Fe–Ti–P alloys as analysed by Leco[®] (LECO Corporation, USA) for oxygen and nitrogen and by Spectrolab (SPECTRO Analytical Instruments GmbH, Germany) for the other elements.

Table 1.

Chemical compositions of the Fe alloys used in the wetting experiments

Sample	Chemical composition of Fe alloys (mass %)								
	C	Si	Mn	P	S	Al	Ti	O _{tot}	N
(a) Titanium samples									
Ti-01	0.0265	0.0046	0.0462	0.0047	0.0070	0.0055	0.0030	0.0035	0.0044
Ti-02	0.0266	0.0059	0.0242	0.0038	0.0046	0.0050	0.0062	0.0067	0.0067
Ti-03	0.0321	0.0042	0.0243	0.0028	0.0054	0.0060	0.0089	0.0078	0.0053
Ti-04	0.0308	0.0036	0.0625	0.0036	0.0047	0.0075	0.0198	0.0067	0.0077
Ti-05	0.0355	0.0040	0.0291	0.0042	0.0100	0.0096	0.0320	0.0057	0.0044
Ti-06	0.0257	0.0043	0.0242	0.0045	0.0035	0.0083	0.0410	0.0025	0.0067
Ti-07	0.0241	0.0070	0.0268	0.0029	0.0048	0.0092	0.0524	0.0039	0.0053
Ti-08	0.0253	0.0032	0.0399	0.0039	0.0043	0.0098	0.0763	0.0024	0.0044
Ti-09	0.0245	0.0032	0.0242	0.0047	0.0050	0.0096	0.0885	0.0027	0.0067
Ti-10	0.0333	0.0083	0.0282	0.0033	0.0047	0.0081	0.0989	0.0087	0.0030
Ti-11	0.0266	0.0039	0.0242	0.0047	0.0031	0.0316	0.1060	0.0049	0.0067
Ti-12	0.0275	0.0049	0.0242	0.0050	0.0032	0.0473	0.1740	0.0046	0.0067
(b) Phosphorus samples									
P-01	0.0381	0.0021	0.0499	0.0034	0.0043	0.0011	0.0013	0.0080	0.0038
P-02	0.0265	0.0014	0.0462	0.0047	0.0070	0.0014	0.0030	0.0045	0.0037
P-03	0.0258	0.0024	0.0322	0.0148	0.0087	0.0013	0.0016	0.0045	0.0043
P-04	0.0387	0.0079	0.0567	0.0181	0.0040	0.0014	0.0015	0.0076	0.0045
P-05	0.0156	0.0019	0.0316	0.0291	0.0095	0.0013	0.0018	0.0045	0.0045
P-06	0.0381	0.0012	0.0574	0.0335	0.0037	0.0010	0.0019	0.0066	0.0046
P-07	0.0383	0.0018	0.0593	0.0454	0.0035	0.0012	0.0021	0.0091	0.0049
P-08	0.0102	0.0019	0.0314	0.0502	0.0086	0.0015	0.0022	0.0045	0.0046
P-09	0.0399	0.0064	0.0380	0.0733	0.0047	0.0011	0.0014	0.0052	0.0042
P-10	0.0159	0.0042	0.0381	0.0751	0.0288	0.0012	0.0026	0.0045	0.0052
P-11	0.0382	0.0068	0.0388	0.0952	0.0042	0.0009	0.0014	0.0049	0.0041
P-12	0.0128	0.0011	0.0429	0.1060	0.0090	0.0009	0.0041	0.0045	0.0056
(c) Samples containing both titanium and phosphorus									
Ti + P-01	0.0402	0.0074	0.0537	0.0034	0.0049	0.0035	0.0102	0.0076	0.0039
Ti + P-02	0.0408	0.0078	0.0625	0.0035	0.0047	0.0071	0.0198	0.0067	0.0077
Ti + P-03	0.0395	0.0072	0.0611	0.0035	0.0044	0.0084	0.0390	0.0063	0.0040
Ti + P-04	0.0348	0.0033	0.0641	0.0224	0.0042	0.0028	0.0445	0.0061	0.0044
Ti + P-05	0.0418	0.0069	0.0649	0.0221	0.0039	0.0022	0.0838	0.0060	0.0040
Ti + P-06	0.0267	0.0085	0.0083	0.0223	0.0031	0.0032	0.1016	0.0049	0.0058
Ti + P-07	0.0278	0.0087	0.0086	0.0220	0.0032	0.0073	0.1427	0.0046	0.0034
Ti + P-08	0.0381	0.0063	0.0391	0.1230	0.0042	0.0051	0.0038	0.0079	0.0043
Ti + P-09	0.0383	0.0087	0.0399	0.1230	0.0043	0.0041	0.0148	0.0084	0.0042
Ti + P-10	0.0386	0.0054	0.0525	0.1230	0.0038	0.0096	0.0378	0.0064	0.0050
Ti + P-11	0.0391	0.0094	0.0410	0.1230	0.0046	0.0061	0.0427	0.0078	0.0039
Ti + P-12	0.0397	0.0023	0.0487	0.1230	0.0038	0.0833	0.0903	0.0080	0.0045

A further step in the preparation involved the cutting of master alloys into cylindrical samples weighing 1.6–1.7 g which were polished, washed in acetone and

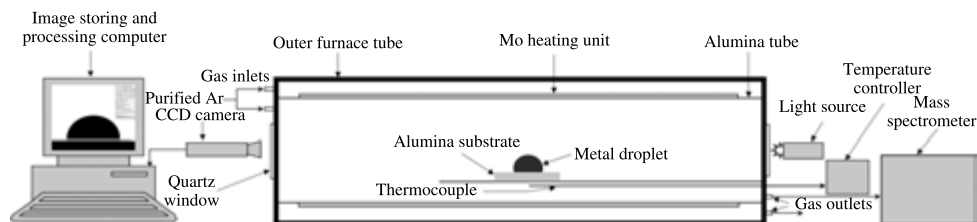


Figure 2. Schematic sketch of the drop shape analysis unit for high temperature wetting measurements [33].

cleaned in an ultrasonic bath for 5 min. After the drying process, the specimen was placed on a clean alumina substrate before being introduced in the furnace. Thereafter, the system was sealed and flushed with Ar gas at a flow rate of 250 ml/min until the oxygen content reached values below 10 ppm as measured by a mass spectrometer on the gas flow exiting the tube furnace.

To eliminate the influence of surface roughness, high purity alumina substrates (99.98 mass % Al_2O_3 , $R_a = 0.2 \mu\text{m}$) were used throughout the experiments.

2.2. Experimental Set-up and Procedure

The wetting experiments were conducted in a laboratory horizontal tube furnace, Fig. 2, under a well controlled atmosphere of ultrahigh purity Ar gas. This gas, initially containing 2 ppm of O_2 and H_2O , was further purified to less than 10 ppb O_2 by passing through an Oxisorb[®] refining system (manufactured by Messer GmbH, Austria) prior to entering the reaction chamber of the furnace.

The heating process was linear at a rate of $15^\circ\text{C}/\text{min}$. A holding time of 10 min at 1620°C was followed by cooling down at a rate of $10^\circ\text{C}/\text{min}$. The temperature was measured by a type B (i.e., Pt30Rh-Pt6Rh) thermocouple located in the immediate vicinity of the sample.

Once the sample was melted, the measurements of the contact angle as a function of temperature and time started. They consisted in a continuous monitoring of the shape of the sessile drop by a digital video camera (25 frames per second) connected to a computer, enabling automatic image analysis using a commercial software. The characteristic dimensions of the droplet (contact angle θ , drop base radius R and height H) were extracted with an accuracy of $\pm 2^\circ$ for θ and $\pm 2\%$ for R and H [34].

2.3. Microscopic Analysis of the Interface

At the end of the wetting experiments, the samples were taken out of the furnace and the interfacial region was analysed microscopically in order to obtain information on the nature of interaction between the substrate and the liquid melt, and the possible formation of reaction products. The chemistry, morphology and microstructure of both sides (metal and substrate) of the interface were determined using a scanning electron microscope (SEM) with energy dispersive X-ray spectroscopy (EDS) facility.

3. Results

The results of the wetting measurements in the Fe–Ti/Al₂O₃ system are presented in Fig. 3. It is clearly seen that the wetting angle decreases greatly with increasing Ti content, most notably in the low concentration range. This is in good agreement with the results of earlier works [35–37], but is not in accord with a relatively recent paper [38], in which the effect of Ti on the wettability of Fe alloys was found to be weak at 1575°C and 1600°C and negligible at 1550°C, Fig. 4.

As expected, droplets of Fe alloys without Ti did not wet alumina, the measured contact angles being greater than 130°. Additions of up to 0.10 mass % Ti led to a remarkable decrease in the steady contact angle to about 90°, and at [Ti] contents greater than 0.15 mass % the Fe alloys were found to become wetting (i.e., $\theta < 90^\circ$).

The non-wetting behaviour observed at very low [Ti] contents is a consequence of the formation at the Fe–Ti/Al₂O₃ interface of an oxide layer. For the oxygen contents expected in the Fe drop, the stable interfacial phase will be hercynite (FeAl₂O₄) which is formed according to the reaction [39]:



The Gibbs free energy of formation ΔG^0 for the above reaction is given by [40]:

$$\Delta G^0 = -328.348 + 82.044 \cdot T \text{ [J} \cdot \text{mole}^{-1}] \text{ (} T \geq 1809 \text{ K)}. \quad (4)$$

At steelmaking temperatures, the value of ΔG^0 is negative, and, therefore, the reaction in equation (3) proceeds spontaneously.

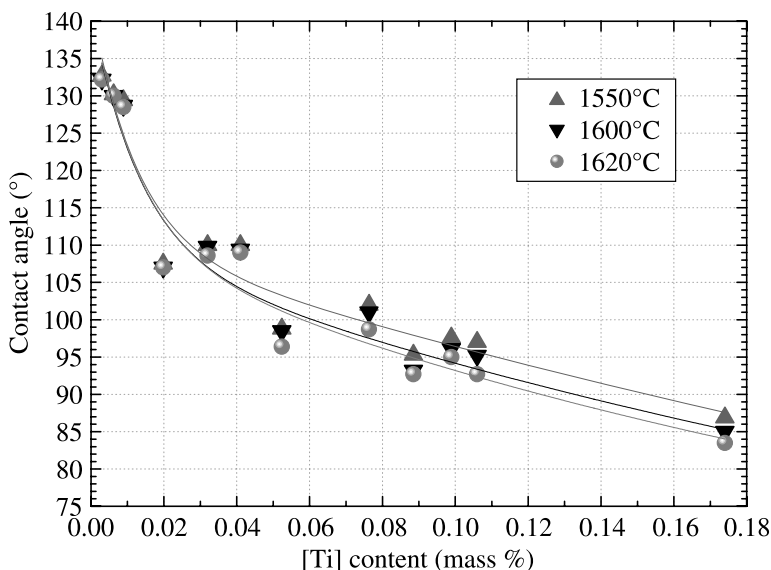


Figure 3. Effect of [Ti] content on the contact angle between Fe–Ti alloys and Al₂O₃ substrates as a function of temperature.

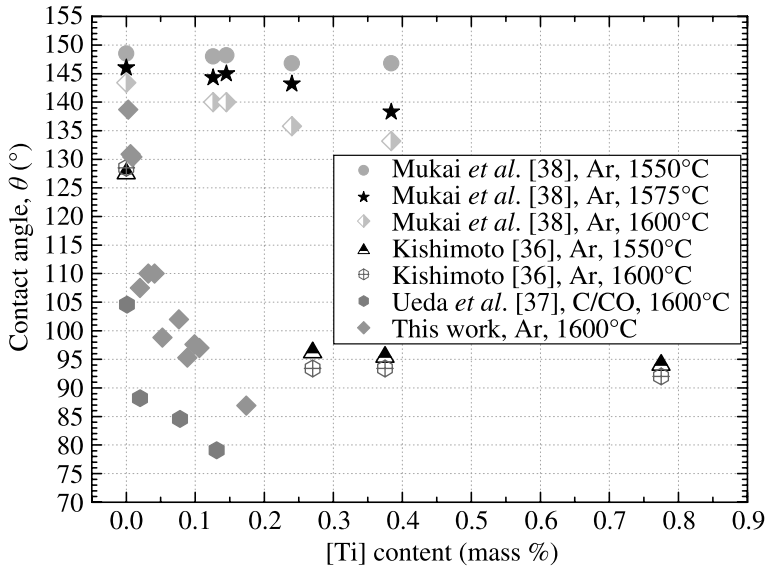


Figure 4. Effect of [Ti] content on the wetting behaviour in the Fe–Ti/Al₂O₃ system: measured contact angles compared with data from literature [35–38]. Next to the authors of the study, the furnace atmosphere and the temperature at which the tests were performed are given.

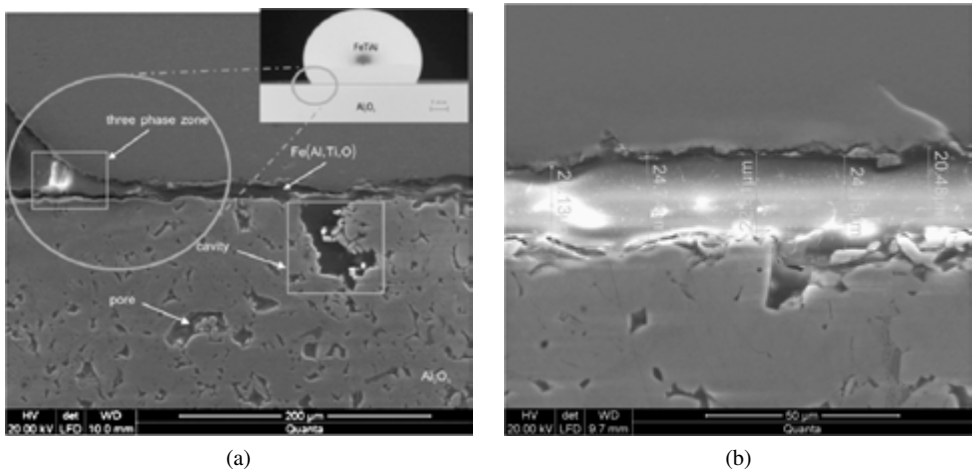


Figure 5. (a) SEM image of cross-section of the interfacial zone after a wetting experiment on the sample Ti-02 with 62 ppm total O and 67 ppm [Ti] showing the formation of a relatively thick interfacial layer composed of complex oxides. Pores and cavities are also seen on the substrate side. A high magnification of the oxide layer in (a) is shown in (b).

After the wetting experiments, the substrate surface under the droplet was completely covered with the reaction product layer, Fig. 5. Nevertheless, the solidified droplet detached easily from the substrate. This implies that the hercynite layer formed is not wetted by liquid Fe. Hence, the equilibrium contact angle θ at

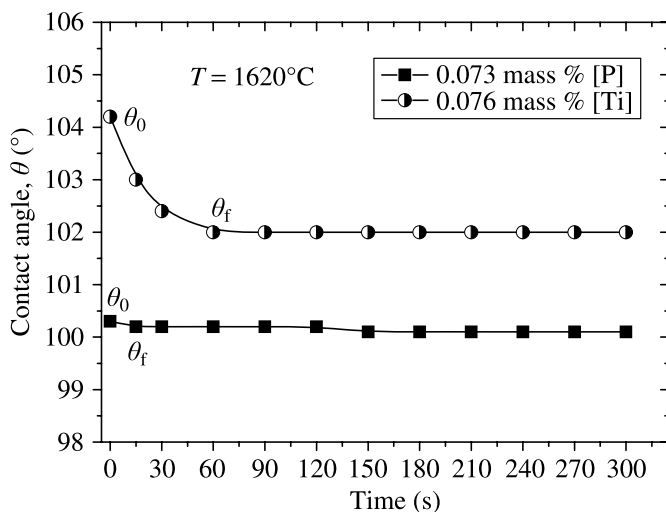


Figure 6. Variation of contact angle with time for Fe–Ti and Fe–P alloys on Al_2O_3 at 1620°C .

the Fe–Ti alloy/ FeAl_2O_4 interface is an obtuse one. An SEM examination of the contact surfaces revealed that after experiments on Fe–Ti alloys with Ti contents <0.1 mass % and low [O] contents, the reaction layer between the droplet and the substrate was rather very thin and consisted only of FeAl_2O_4 , while in the case of the experiments under high [Ti] contents this layer was thicker and rich in Al, O, Fe and Ti. In the latter case, the Fe–Ti droplet adhered firmly to the underlying substrate, which is another clear indication that an interfacial reaction had occurred. The current finding is consistent with the work by Nakashima *et al.* [21].

Although the measurement results show that the influence of temperature on the wetting behaviour in this system is not very significant, it is interesting to notice that it is less pronounced at lower [Ti] contents as illustrated in Fig. 3. As a general trend though, a slight improvement in wettability is registered at higher temperatures.

As for the spreading kinetics, it was observed that the equilibrium contact angle θ_f was reached within a few seconds for Fe–P samples, whereas for Fe–Ti samples it took up to 60 s to attain the value of θ_f , Fig. 6.

In the case of Fe–P samples, it was found that the wetting angles exhibited a marked decrease with increasing [P] concentration in the melt composition, Fig. 7, but the improvement in wettability was moderate as compared to that observed in the Fe–Ti series. Additional alloying to [P] contents above 0.10 mass % did not contribute to any further decrease of the contact angle which remained obtuse in the investigated concentration range.

The SEM analysis of the P samples after the experiments showed that, unlike in the case of Ti, there was no hercynite reaction layer between the droplet and the substrate. Instead, cracks formed at the spreading front, Fig. 8. According to

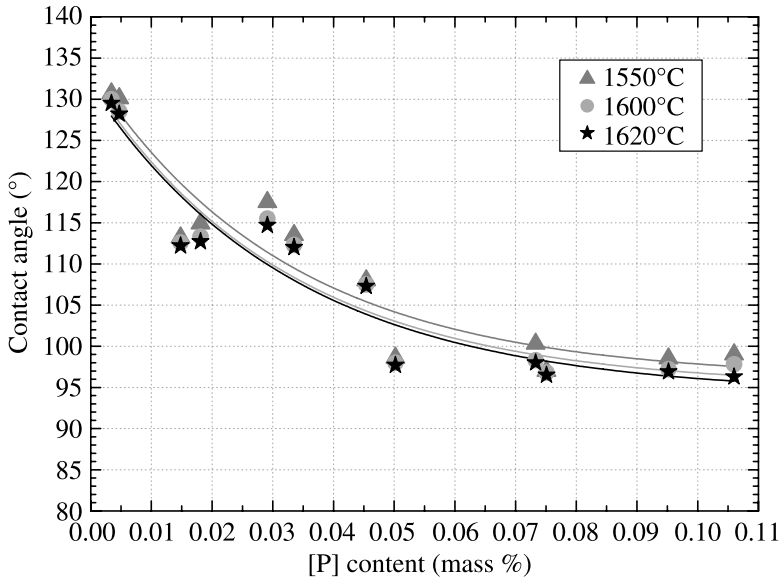


Figure 7. Effect of [P] content on the wetting angle between Fe–P alloys and Al_2O_3 substrates as a function of temperature. The temperature influence on the wetting behaviour is almost constant for all investigated temperature values.

Novotny [41], the crack formation results from the large coefficient of thermal expansion mismatch exhibited by almost all metal/ceramic couples which leads to thermal stresses during the spreading process.

Following the occurrence of cracks, the molten Fe alloy can penetrate along these cracks to react with the bulk Al_2O_3 substrate, with the net effect of a progressive decrease in the drop height (volume) and the contact angle [42]. On the other hand, the presence of a crack could, in a similar way to the ‘pinning effect’ of a ridge [24, 26], act as a wetting barrier in obstructing and eventually stopping the advance of the spreading front, with the consequence of a poor wetting. Both effects being diametrically opposed, their balance determines the actual influence of cracks on the wetting behaviour in the Fe–P/ Al_2O_3 system [43].

Finally, the combined effect of Ti and P on the wetting behaviour in Fe melts was found not to be additive, but at best partially synergetic. The curves in Fig. 9 clearly show that at low [P] contents in the Fe alloy, changes in contact angle follow almost the pattern observed in Fig. 3, in which the θ values decreased exponentially with increasing [Ti] content irrespective of the [P] concentration. At high P contents, however, the wettability depends largely on the [P] concentration in the melt.

With regard to the SEM/EDS analysis, the results obtained after the experiments with samples containing Ti and P simultaneously revealed the existence of an interfacial hercynite layer which was, however, thinner compared to one observed in the case of Fe–Ti alloys.

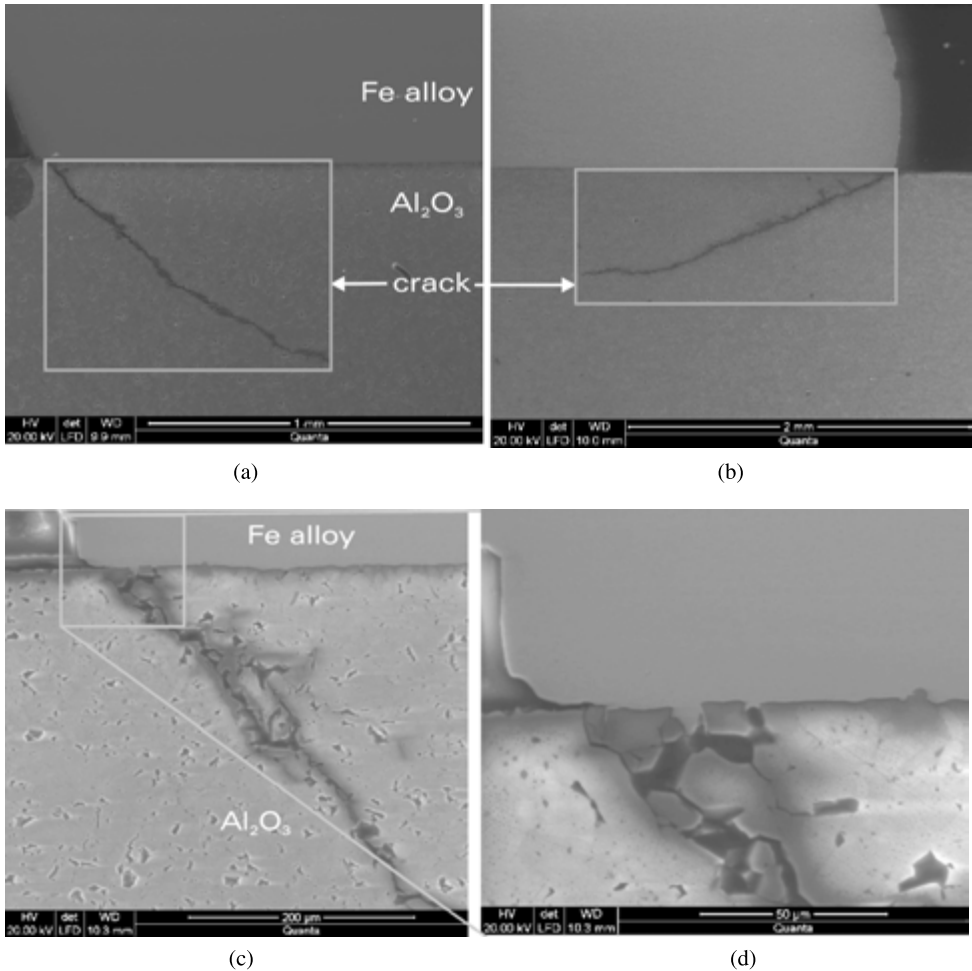


Figure 8. SEM images of the interfacial zone after the wetting experiment on the sample P-08 with 45 ppm total O and 500 ppm [P]. The formation of cracks at the solid–liquid interfacial front is observed on both sides of the contact line as shown in images (a) and (b). High magnifications of the crack in (a) are given in (c) and (d). They show the disintegrated ceramic substrate filled with the Fe alloy melt, indicating a good wetting between the melt and Al₂O₃. As a result, the solidified metal droplet was tightly bonded to the substrate.

4. Discussion and Interpretation of Results

Due to the addition of small amounts of Ti (<0.2 mass %) a decrease in the final contact angle from 133° to 85° was observed in our experiments, Fig. 3. It has been suggested that the addition of reactive elements such as Ti to the liquid Fe alloy improves the wetting on ceramics due to the formation of an interfacial reaction layer [14], which was confirmed in this work.

In the liquid Fe–Ti/Al₂O₃ system, reactivity depends critically on the concentrations of both titanium and oxygen in the alloy, as the actual O₂ potential is

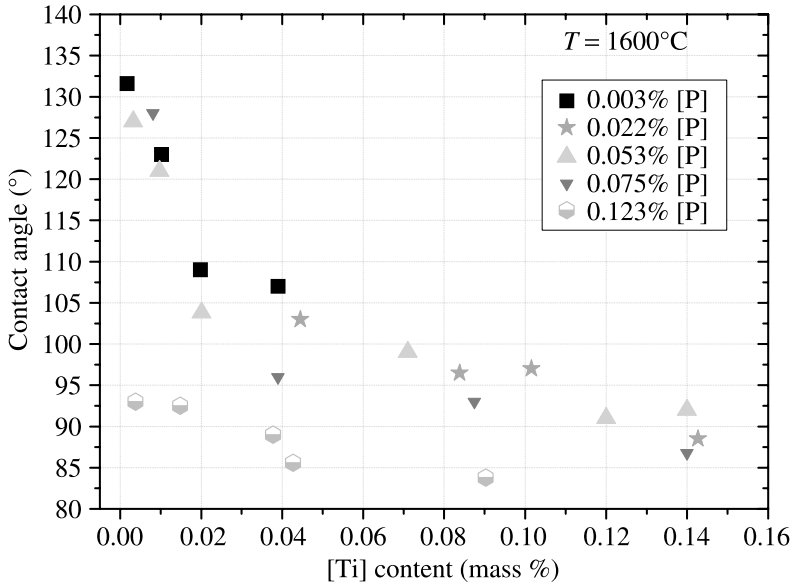
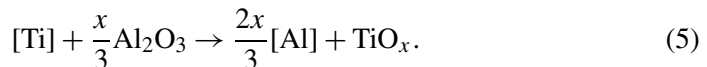


Figure 9. Combined effect of [Ti] and [P] contents on the contact angle between Fe–Ti–P alloys and Al_2O_3 substrates at 1600°C .

determined by the kinetics of the reaction between Ti and O and the dissolution of the Al_2O_3 substrate [44]. In the metallurgical practice, the addition of titanium to a Fe melt in contact with an alumina refractory results in reactions involving the dissolution of Al_2O_3 according to the following general equation [45]:



As a result of this reaction, the melt gets enriched in ‘interface active’ Al and various Ti oxides, some of which are wetted by liquid Fe, are formed. This is a potential mechanism that drives reactive wetting in a low O content gas atmosphere where the Fe droplet wets alumina due to reaction (5) [21]. Thus, at low [Ti] concentrations, reactivity involves some but limited dissolution of Al into the alloy, whereas at high [Ti] contents, Ti reacts with Al_2O_3 to form wettable TiO_x layers of the order of some micrometers in thickness at the interface. The change in the nature of the alloy/substrate interface, from Fe–Ti/ Al_2O_3 to Fe–Ti/ TiO_x , leads to a pronounced change in wetting (from contact angles much higher than 130° to contact angles in the $80\text{--}90^\circ$ range).

The spreading rate is found to depend strongly on Ti activity in the alloy, indicating a reaction-induced process. The experimental results are in good agreement with the approach to reactive wetting proposed by Eustathopoulos *et al.* [14], according to which both the final degree of wetting and the spreading rate are controlled by the interfacial reaction product. This was confirmed by the observation of the wetting kinetics through the examination of videos taken during the experiments. During

the first few seconds, no spreading of the alloy was observed while the temperature was raised at a constant rate of 15°C/min. The contact angle of about 130° observed at this stage is typical of non-reactive metal/oxide systems [14, 27]. The sudden spreading appears to be triggered by Ti reaching the triple line by diffusion from the bulk of the droplet.

From thermodynamic considerations, Kim *et al.* [46] concluded that Ti exists in the form of a binary $\text{TiO}_x\text{--Al}_2\text{O}_3$ phase in the inclusions observed in Ti-bearing Al-killed low carbon steels. The $\text{TiO}_x\text{--Al}_2\text{O}_3$ inclusions are reported to be wetted more easily by the liquid Fe compared to the pure Al_2O_3 inclusions [9, 45]. In the case of TiO_x (i.e., Ti oxides of varying oxidation states), reported values of the contact angle for TiO_2 with liquid Fe vary between 84° [18] and 80° [47]. As a result of these low θ values, the separation of TiO_x inclusions at the steel/slag interface is unlikely.

The results of SEM analysis revealed that the Ti oxides segregated at the surface of the steel droplet as well as at the interface between the droplet and the alumina substrate, thus causing dramatic decreases in the contact angle. This suggests that these oxides are surface active with respect to Fe melts.

The above discussed results help to understand the reasons for the frequent nozzle clogging experienced during the casting of Fe–Ti alloys. Accordingly, under the condition where the re-oxidation rate is controlled at a low level, the effect of Ti addition to liquid steel is to increase the wetting of alumina by the steel melt. Thus, a better contact between the refractory material of the submerged entry nozzle and the steel melt would follow, resulting in an increased cooling rate at the steel/nozzle interface, and subsequently in the occurrence of the thermal clogging manifested by freezing of steel at the melt/refractory interface. These results corroborate the view expressed by other research groups [8, 9, 37].

Considering the influence of phosphorus, the improvement in the wetting behaviour of P bearing Fe alloys on alumina substrates cannot be attributed to the formation of a continuous reaction product layer at the metal/alumina interface. At investigated P contents, a decrease in contact angle with increasing [P] content was registered but no reaction layer containing P was observed. Instead, metallographic investigations performed on the solidified droplet sample and the substrate revealed the existence of small islands of a reaction product rich in P in the close vicinity of the triple line. This is in agreement with the theory stating that the decrease in contact angle can be explained by the adsorption of the alloying element at the solid/liquid interface [14]. These findings are also supported by the work of Xue *et al.* [48], in which P in liquid Fe was found to act as a surface active element and to segregate extensively on the surface of Fe alloys. Moreover, P is known to considerably enhance the oxygen activity in the Fe melt [49]. Thus, P additions to Fe-based melts do modify significantly the liquid–vapour surface tension of the system.

The time dependence of the contact angle in the Fe–P/ Al_2O_3 couple shows that the stable values of θ are established within seconds. This is partly due to the fact that P lowers the viscosity of the steel melt, thus accelerating the wetting kinetics

[4, 25]. The rapid establishment of the equilibrium θ suggests that we are dealing with a non-reactive system.

During the experiments on Fe–Ti–P melts, it was found that the effect of Ti and P together on the wetting behaviour is not additive. Ti, being the most surface active element, concentrates itself at the interfaces and, consequently, leads to a decrease of γ_{sl} and/or γ_{lv} . As the experimental results showed, at least at high [P] contents (>0.1 mass %), an increase in [Ti] content does not contribute significantly to wetting in spite of the precipitation of Ti at the interface. The positive effect of P on wetting is due to its role in enhancing the Ti activity in the Fe melt [4].

5. Conclusions

In this study we have investigated the wetting behaviour of Al_2O_3 by Fe–Ti and Fe–P alloys as a function of alloy chemical composition, temperature and time. The main findings can be summarised as follows:

- In light of our experimental data, it is expected that the wetting behaviour of Fe melts alloyed with Ti and/or P will depend on both the nature and quantity of the alloying element and the abundance of dissolved oxygen.
- In binary Fe–Ti alloys, wetting increases considerably with increasing [Ti] content, and moderately with temperature. The alloys react with Al_2O_3 at the interface to form a complex layer of oxides composed of $FeAl_2O_4$ and TiO_x . The slight variation of wetting angle with time results from the high interfacial reactivity due to the presence of Ti.
- The Fe–P/ Al_2O_3 couple is a non-wetting system in which the wetting angle decreases substantially with increasing [P] concentration. The initial transient wetting angles do not vary significantly with temperature and time, and the final equilibrium is established between the Fe–P melt and the initial Al_2O_3 substrate. The improvement of wettability in this system is due to the surface adsorption effect of P which contributes to a decrease in γ_{lv} .
- The effect of Ti and P together on the wetting behaviour of Fe alloys on Al_2O_3 is not additive. The effect of P on Ti bearing steels consists mainly in enhancing the activity of Ti in the melt, thus resulting in a reduction of the threshold [Ti] concentration needed to obtain a given level of wetting.
- With regard to adhesion, it was observed that a good wettability is no prerequisite for a strong adhesion: As our study showed, a strong bond of the Fe melt to the Al_2O_3 substrate was achieved even though the measured values of θ were well above 90° .

Clearly, this research has only been able to touch on some aspects of the complex topic of high-temperature wetting. In order to validate and complete the work car-

ried out, a more in-depth investigation aimed at quantifying the effects of various interrelated factors on reactive wetting would be useful.

Acknowledgements

This research was carried out within the framework of a project co-financed by the Christian Doppler Research Association and voestalpine Stahl Linz.

References

1. K. C. Mills and S. Sridhar, in: *Proc. Belton Memorial Symposium*, Sydney, pp. 211–226 (2000).
2. J. Strandh, K. Nakajima, R. Eriksson and P. Jönsson, *ISIJ Int.* **45**, 1597–1606 (2005).
3. K. Rackers and B. G. Thomas, in: *Proc. of the 78th Steelmaking Conf.*, Vol. 78, pp. 723–734 (1995).
4. Y. Kawai and Y. Shiraishi (Eds), *Handbook of Physico-Chemical Properties at High Temperatures*. The Iron and Steel Institute of Japan, Tokyo (1988).
5. M. Humenik and W. D. Kingery, *J. Am. Ceram. Soc.* **37**, 18 (1954).
6. K. Ogino, A. Adachi and K. Nogi, *Tetsu-to-Hagane* **59**, 1237 (1973).
7. P. Kozakevitch and L. D. Lucas, *Rev. Metall.* **65**, 589 (1988).
8. B. J. Keene, *Intl. Mater. Rev.* **33**, 1 (1988).
9. S. Basu, S. K. Choudhary and N. U. Girase, *ISIJ Int.* **44**, 1653–1660 (2004).
10. T. Young, *Phil. Trans. R. Soc. London* **95**, 65 (1805).
11. H. J. Butt, K. Graf and M. Kappl, *Physics and Chemistry of Interfaces*, 2nd edn. Wiley, Weinheim, Germany (2006).
12. M. Schick, in: *Liquids at Interfaces*, J. Charvolin, J. F. Joanny and J. Zinn-Justin (Eds), pp. 415–489. Elsevier, Amsterdam (1988).
13. S. Hartland, *Surface and Interfacial Tension: Measurement, Theory, and Applications*. Marcel Dekker, New York (2004).
14. N. Eustathopoulos, M. G. Nicholas and B. Drevet, *Wettability at High Temperatures*, 1st edn. Pergamon, Amsterdam (1999).
15. K. C. Mills, E. D. Hondros and Z. Li, *J. Mater. Sci.* **40**, 2403–2409 (2005).
16. A. W. Cramb and I. Jimbo, *Iron and Steelmaker* **16**, 43–55 (1989).
17. R. F. Brooks and P. N. Queded, *J. Mater. Sci.* **40**, 2233–2238 (2005).
18. M. Kudoh, K. Ohsasa, K. Tanaka and K. Okuyama, *Bull. Faculty Eng., Hokkaido University* **162**, 191–202 (1992).
19. C. Wan, P. Kritsalis, B. Drevet and N. Eustathopoulos, *Mater. Sci. Eng., A* **207**, 181–187 (1996).
20. J. G. Li, *Ceram. Int.* **20**, 391–412 (1994).
21. K. Nakashima, K. Takihira, K. Mori and N. Shinozaki, *Mater. Trans., JIM* **33**, 918–926 (1992).
22. S. Ueda, H. Shi, X. Jiang, H. Shibata and A. W. Cramb, *Metall. Mater. Trans. B* **34**, 503–508 (2003).
23. N. Rauch, High temperature spreading kinetics of metals, *PhD Thesis*, University Stuttgart, Germany (2005).
24. E. Saiz, A. P. Tomsia and R. M. Cannon, *Acta Mater.* **46**, 2349–2361 (1998).
25. A. Carré and M. E. R. Shanahan, *Langmuir* **11**, 24 (1995).
26. V. de Jonghe and D. Chatain, *Acta Metall. Mater.* **43**, 1505–1515 (1995).
27. A. Carré, J. C. Gastel and M. E. R. Shanahan, *Nature* **379**, 432 (1996).

28. G. Kaptay and E. Bader, *Trans. Joining and Welding Research Inst.* **30**, 55–60 (2001).
29. R. Asthana and N. Sobczak, *JOM* **52**, 1 (2000). Available at <http://www.tms.org/pubs/journals/JOM/0001/Asthana/Asthana-0001.html>.
30. P. Kritsalis, B. Drevet, N. Valignat and N. Eustathopoulos, *Scripta Metall. Mater.* **30**, 1127 (1994).
31. K. Landry, C. Rado and N. Eustathopoulos, *Metall. Mater. Trans. A* **27**, 318 (1996).
32. K. Landry, C. Rado, R. Voitovich and N. Eustathopoulos, *Acta Mater.* **45**, 3079 (1997).
33. C. Bernhard, A. Karasangabo, H. Presslinger and P. Reisinger, in: *Proc. of the 2nd CSM-VDEh Seminar on Metallurgical Fundamentals*, Düsseldorf, pp. 219–232 (2007).
34. Kruess GmbH, *DSA User Manual*, Hamburg (2003).
35. B. T. Eldred and P. D. Ownby, *Trans. Joining and Welding Research Inst.* **30**, 69–74 (2001).
36. M. Kishimoto, K. Mori and Y. Kawai, *J. Jpn. Inst. Metals* **48**, 413 (1984).
37. S. Ueda, H. Shi and A. W. Cramb, *Steel Grips* No. 2, 53–56 (2004).
38. K. Mukai, L. Zhong and M. Zeze, in: *Proc. of the 12th ISIJ-VDEh Seminar*, Kitakyushu, Japan, pp. 177–184 (2005).
39. B. Deo and R. Boom, *Fundamentals of Steelmaking Metallurgy*. Prentice Hall International, London, UK (1993).
40. I. Barin, *Thermodynamical Data of Pure Substances, Parts I and II*. VCH, Weinheim, Germany (1993).
41. J. Novotny, in: *Materials Science Monographs*, Vol. 75. Elsevier, Amsterdam (1991).
42. P. Shen, H. Fujii, T. Matsumoto and K. Nogi, *Metall. Mater. Trans. A* **35**, 583–587 (2004).
43. A. Karasangabo, Wetting and interfacial reaction investigations of iron-based alloys/alumina systems by means of the sessile drop shape analysis method, *PhD Thesis*, Department of Metallurgy, Leoben University, Austria (2009).
44. W. Y. Kim, J. O. Jo, C. O. Lee, D. S. Kim and J. J. Pak, *ISIJ Int.* **48**, 17–22 (2008).
45. J. Lehmann and H. Gaye, in: *Proc. of the 82nd Steelmaking Conf.*, pp. 463–470 (1999).
46. D. S. Kim, H. S. Song, Y. D. Lee, Y. Chung and A. W. Cramb, in: *Proc. Steelmaking Conf.*, ISS-AIME, pp. 399–416 (1997).
47. S. Ogibayashi, *Taikabutsu Overseas — J. Techn. Association of Refractories* **15**, 22 (1995).
48. X. M. Xue, H. G. Jiang, Z. T. Sui, B. Z. Ding and Z. Q. Hu, *Metall. Mater. Trans. B* **27**, 71–79 (1996).
49. S. Seetharaman, *Fundamentals of Metallurgy*. Woodhead Publishing Limited, Cambridge, UK (2005).
50. M. E. R. Shanahan, *J. Phys. D: Appl. Phys.* **20**, 945–950 (1987).